Nitrogen-Vacancy Centers in Diamond For Quantum Sensing

Robin Teng

Electrical and Computer Engineering Department, University of California, Santa Barbara

Abstract

Diamonds might be famous for their flawless clarity, but in thse realm of quantum device engineering, their true value actually lies in their imperfections. This report serves as a comprehensive overview of my research topic: color centers in diamond, with a specific focus on the Nitrogen-Vacancy (NV) center. Operating essentially as an "artificial atom" trapped within a robust carbon lattice, the NV center provides an unprecedented platform for room-temperature quantum sensing. By leveraging a mechanism known as Optically Detected Magnetic Resonance (ODMR), we can use a combination of laser excitation and microwaves to read the quantum spin states of these defects, effectively translating atomic-scale physics into highly sensitive magnetic measurements. In the following sections, we will break down the underlying physics that make this transduction possible, explore practical applications ranging from nanoscale biosensing to GPS-denied magnetic navigation, and address the current nanofabrication and material challenges that engineers must overcome to bring this technology out of the lab and into the real world.

1. BACKGROUND: DIAMOND AND DEFECT PHYSICS

1.1. Material Properties of Diamond

While famous in jewelry for its brilliant total internal reflection, driven by a remarkably high refractive index ($n \approx 2.4$), diamond is fundamentally a wide-bandgap (5.5 eV) semiconductor. Structurally, the crystal consists of two interpenetrating face-centered cubic (FCC) lattices transposed exactly on top of one another. Within this dense matrix ($a_0 = 0.357$ nm), every carbon atom forms four exceptionally strong sp^3 covalent bonds with its nearest neighbors, as illustrated in Fig. 1.

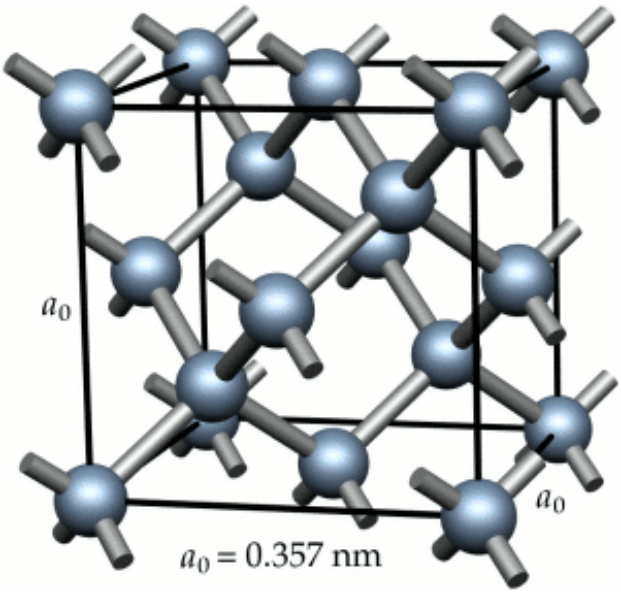

Figure 1. The diamond cubic crystal structure, composed of two interpenetrating FCC lattices with sp^3 bonding.

This immense structural rigidity and uniform bonding are the secrets to diamond's outstanding quantum properties. A critical metric in any quantum system is its coherence time: the duration a quantum state (such as an electron spin) can exist before it is scrambled by environmental disruptions. Because the stiff carbon lattice is highly resistant to thermal vibrations, it acts as a protective vault, shielding internal quantum states from thermal noise. Consequently, diamond-hosted quantum systems can maintain their coherence for exceptionally long periods, even at room temperature.

1.2. Color Centers and Artificial Atoms

No material is perfectly pure. In diamond, microscopic impurities and structural flaws are known as "color centers" because they are responsible for the vibrant hues seen in natural diamonds. Crucially, these defect structures also allow the diamond to fluoresce under optical illumination, a property essential for the sensing techniques discussed later.

While these crystal imperfections can take several forms, such as foreign impurities or extra atoms squeezed into the matrix, this report is primarily concerned with vacancies, where a carbon atom is simply missing from the lattice, as illustrated in Fig. 2.

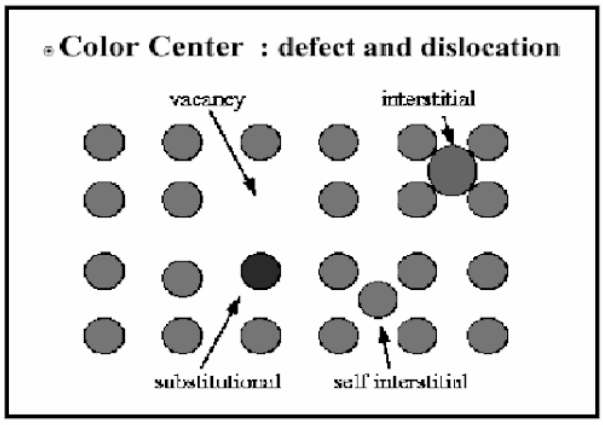

Figure 2. Common types of crystal defects in diamond, including substitutional impurities and lattice vacancies.

Because the rigid diamond lattice tightly confines the electrons trapped within these specific flaws, they behave exactly like isolated "artificial atoms." Scientists have engineered a variety of these color centers, such as Silicon-Vacancy (SiV), Tin-Vacancy (SnV), and Nickel (Ni) variants, for highly specific quantum tasks like quantum memory or as Single Photon Emitters (SPEs).

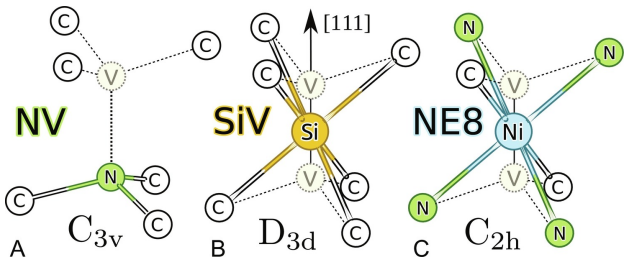

Figure 3. A selection of engineered color centers in diamond, each offering distinct optical and spin properties for quantum applications.

While these alternative color centers hold incredible promise, this review will focus exclusively on the Nitrogen-Vacancy (NV) center, which has emerged as the premier candidate due to its longer spin coherence time at room temperature for quantum sensing.

2. PHYSICS OF THE NITROGEN-VACANCY (NV) CENTER

2.1. Atomic Structure and Symmetry

The Nitrogen-Vacancy (NV) center forms when a substitutional nitrogen atom pairs with an adjacent carbon vacancy in the diamond lattice. Due to the tetrahedral bonding of the surrounding carbon atoms, the axis connecting the nitrogen and the vacancy sits at a characteristic 109.5° angle, as shown in Fig. 4.

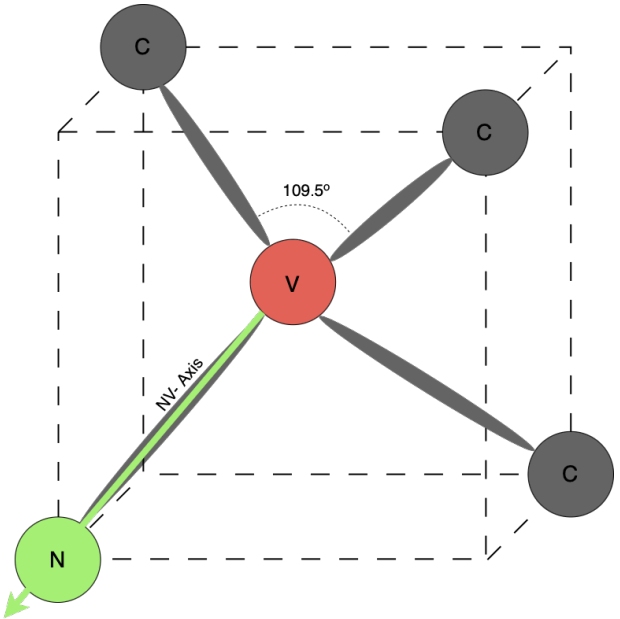

Figure 4. Atomic structure of the negatively charged NV^- center in diamond, showing the nitrogen atom paired with an adjacent carbon vacancy.

This specific spatial arrangement gives the defect a C_{3v} point group symmetry, which fundamentally dictates the defect's allowable energy levels, optical transitions, and spin dynamics. Depending on the local electronic environment, such as nearby impurities that act as electron donors, the NV center stabilizes into one of three distinct charge states, summarized in Table 1.

Table 1. Stable Charge States of the NV Center

Charge State	Notation	Electrons	Quantum Utility
Positive	NV^+	4	Optically inactive; not utilized for quantum applications.
Neutral	NV^0	5	Optically active, but lacks the necessary spin properties.
Negative	NV^-	6	Primary active state; forms the readable spin system essential for quantum sensing.

Note: Almost all quantum engineering focuses exclusively on the NV^- state.

Because the NV^+ and NV^0 states lack the required spin characteristics, almost all quantum engineering focuses exclusively on the negative NV^- state. To understand why this specific state acts as a quantum sensor, we must examine how its six electrons arrange themselves within the defect.

2.2. Electron Structure and Orbital Configuration

To understand the NV^- center as a quantum sensor, we must first account for its six electrons. These originate from the three adjacent carbon dangling bonds, two from the nitrogen atom's lone pair, and one extra captured from the surrounding lattice environment, often donated by a nearby neutral nitrogen impurity. This final captured electron is what gives the center its stable negative charge.

Within the vacancy's potential well, these electrons arrange themselves into molecular orbitals dictated by the defect's C_{3v} symmetry. The first four electrons completely fill the lower-energy a_1 orbitals. Because these levels are fully occupied by spin-paired electrons, their net magnetic moment cancels out to zero, these four electrons are effectively "locked" in closed shells and do not actively participate in the center's quantum dynamics, as illustrated in Fig. 5.

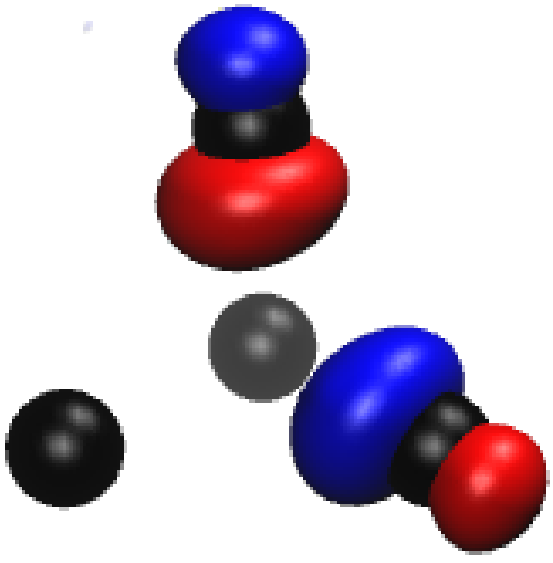

Figure 5. Orbital configuration of the NV^- center, showing the filled a_1 orbitals and the two active electrons occupying the degenerate e_x and e_y orbitals.

With the first four electrons magnetically silent, the remaining two electrons are forced into the higher-energy, degenerate e_x and e_y orbitals. This physical reality allows the complex many-body physics of the NV^- center to be elegantly simplified. From an engineering perspective, the closed inner shells can be ignored, allowing us to treat the defect entirely as a two-electron system governed exclusively by these final two active electrons.

2.3. Spin States In NV Centers

With the NV center simplified to a two-electron system, these active electrons align into four distinct quantum configurations. Following Hund's Rule, they preferentially align with parallel spins, creating a total spin angular momentum of $S = 1$. This forms a spin "triplet" ground state of three symmetric configurations:

$$|T_{+1}\rangle = |\uparrow\uparrow\rangle, \quad m_s = +1 \tag{1}$$

$$|T_{-1}\rangle = |\downarrow\downarrow\rangle, \quad m_s = -1 \tag{2}$$

$$|T_0\rangle = \frac{1}{\sqrt{2}}(|\uparrow\downarrow\rangle + |\downarrow\uparrow\rangle), \quad m_s = 0 \tag{3}$$

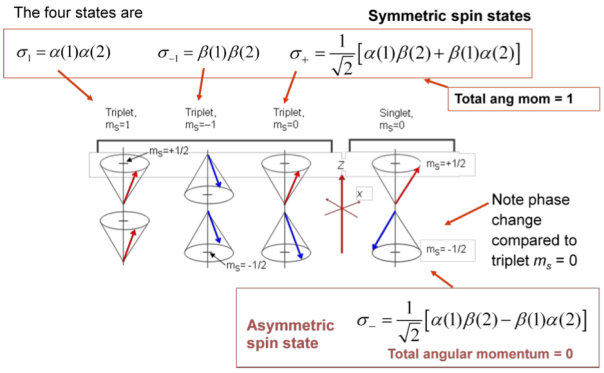

Figure 6. The four spin configurations of the two-electron system in the NV⁻ center: three symmetric triplet states and one antisymmetric singlet state.

The fourth configuration is the spin "singlet" state ($S = 0$), denoted as:

$$|S_0\rangle = \frac{1}{\sqrt{2}}(|\uparrow\downarrow\rangle - |\downarrow\uparrow\rangle), \quad m_s = 0 \tag{4}$$

While both $|T_0\rangle$ and $|S_0\rangle$ share a spin projection of $m_s = 0$, they are fundamentally distinct. The triplet $|T_0\rangle$ is a symmetric state, whereas the singlet $|S_0\rangle$ is an antisymmetric spin state, defined by a negative phase between the basis vectors. Because quantum selection rules require the conservation of total spin, direct optical transitions between the $S = 1$ triplet and $S = 0$ singlet are strongly forbidden. This energetic isolation is what allows the NV center to operate as a highly stable, controllable quantum system.

3. OPTICALLY DETECTED MAGNETIC RESONANCE(ODMR)

3.1. Optical Fluorescence

To interact with the NV center's spin, the system is continuously illuminated by a green laser, typically at a wavelength of 532 nm. A higher-energy green laser is required, rather than a red one, to ensure the electrons absorb enough energy to be efficiently pumped from the ground state high into the phonon bands of the excited state. When these electrons subsequently relax back down to the ground state, they emit broadband red fluorescence centered around 700 nm.

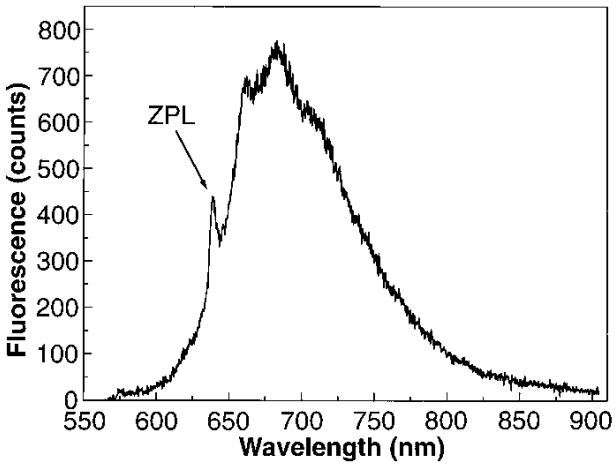

Figure 7. Emission spectrum of the NV⁻ center, showing the sharp Zero-Phonon Line (ZPL) at 637 nm accompanied by a broad phonon sideband extending toward 900 nm. (Gruber et al., 1997)

As shown in Fig. 7, this fluorescence features a sharp Zero-Phonon Line (ZPL) at exactly 637 nm, accompanied by a much broader phonon sideband stretching toward 900 nm, caused by the optical transition coupling with the natural thermal vibrations of the diamond lattice.

The defining feature of the NV center is that the intensity of this red fluorescence is strictly dependent on the electron's spin state, as illustrated by the energy level diagram in Fig. 8.

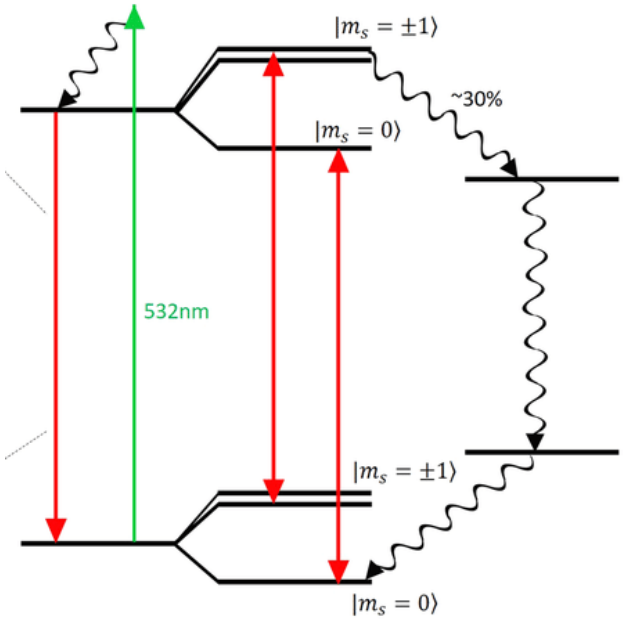

Figure 8. Energy level diagram of the NV⁻ center showing the spin-dependent relaxation pathways for the $m_s = 0$ and $m_s = \pm 1$ states, including the non-radiative intersystem crossing through the dark singlet state. (Ma et al., 2019)

When the active electrons are in the symmetric $m_s = 0$ state, transitioning to the asymmetric dark singlet state is quantum mechanically forbidden. As a result, the $m_s = 0$ state experiences near-unity radiative recombination; the electrons fall directly back to the ground state and emit a bright red photon.

Conversely, when the electrons are in the $m_s = \pm 1$ states, quantum selection rules permit an alternative relaxation pathway. These electrons can undergo phonon scattering, an intersystem crossing, into the dark singlet state, and then non-radiatively decay back to the ground state without emitting any red light. Because this non-radiative decay is a highly probabilistic process, the overall fluorescence collected

drops significantly. Ultimately, an NV center in the $m_s = \pm 1$ state appears approximately 30% dimmer than one in the $m_s = 0$ state.

This ~30% optical contrast is the linchpin of diamond quantum sensing. It provides a direct mechanism to translate an invisible quantum spin state into a macroscopic, easily measurable shift in light intensity, a capability that forms the exact foundation for detecting external magnetic fields.

3.2. ODMR setup

To actively manipulate and read these spin states, engineers use Optically Detected Magnetic Resonance (ODMR). A typical setup uses a 532 nm green laser to excite the diamond. A dichroic mirror separates the incoming laser from the returning red fluorescence, directing the emitted photons to a single-photon counting module (SPCM). Simultaneously, a microwave antenna adjacent to the sample delivers an amplified radio-frequency signal to manipulate the electron spins.

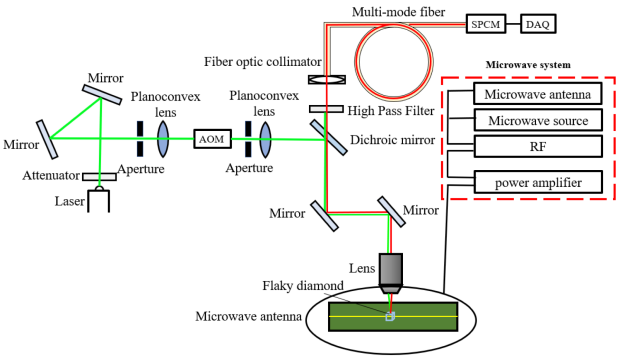

Figure 9. Schematic of a typical ODMR experimental setup, showing the 532 nm excitation laser, dichroic mirror, microwave antenna, and single-photon counting module (SPCM). (Fan et al., 2024)

Before performing any measurements, it is crucial to isolate an individual defect. By raster-scanning the laser across the diamond, researchers generate a photoluminescence (PL) map to pinpoint highly localized spots of red emission. To guarantee that the signal originates from exactly one NV center rather than a dense cluster, a $g^{(2)}$ autocorrelation measurement is performed. A distinctive dip in the $g^{(2)}$ plot confirms single-photon emission, ensuring the sensor's nanoscale spatial resolution, often yielding a highly focused optical spot with a Full Width at Half Maximum (FWHM) of around 430 nm.

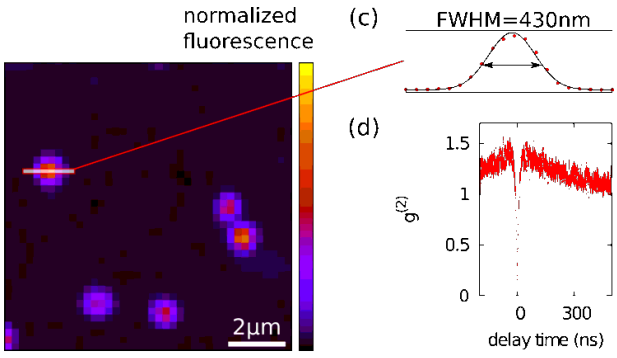

Figure 10. Photoluminescence (PL) map of an NV center in diamond (left) and the corresponding $g^{(2)}$ autocorrelation measurement (right), confirming single-photon emission from an isolated defect.

Once isolated, the antenna sweeps through a range of microwave frequencies. At zero magnetic field, the spin-spin interaction between the two active electrons produces a zero-field splitting parameter $D \approx 2.87$ GHz, the energy gap between the bright $m_s = 0$ state and the dark $m_s = \pm 1$ states. When the applied microwaves match this resonant frequency, the electrons absorb the energy and undergo a spin flip, forcing them into the non-radiative $m_s = \pm 1$ states. This manifests as a sharp ~30% drop in collected fluorescence. This controllable intensity drop forms the baseline for ODMR, setting the stage for highly sensitive magnetic field detection.

3.3. Zeeman Splitting and Vector Magnetometry

While ODMR provides the optical readout mechanism, it is the Zeeman effect that actually enables the NV center to function as a magnetic sensor. At zero magnetic field, the $m_s = \pm 1$ states are degenerate, resulting in a single ODMR resonance dip at approximately 2.87 GHz. However, when an external magnetic field B is introduced, the Zeeman effect breaks this degeneracy. The magnetic field interacts with the electron's magnetic moment, causing an energy shift defined by the Electron Zeeman Interaction:

$$E = m_s \, g \, \mu_B \, B_{\parallel} \tag{5}$$

where m_s is the spin quantum number, g is the Landé g-factor ($g \approx 2$ for the NV center), μ_B is the Bohr magneton, and $B_{\parallel}$ is the magnetic field component parallel to the NV axis. This causes the energy level of the $m_s = +1$ state to rise and the $m_s = -1$ state to fall, splitting the single resonance dip into two distinct dips.

In an ODMR spectrum, this energy gap is measured as a frequency separation $\Delta\nu$ between the two peaks. Because the NV center only responds to the magnetic field projection parallel to its symmetry axis, the observable frequency split is governed by the angle θ between the NV axis and the external field:

$$\Delta\nu = 2\gamma B \cos(\theta) \tag{6}$$

where γ is the electron gyromagnetic ratio ($\gamma \approx 28$ GHz/T).

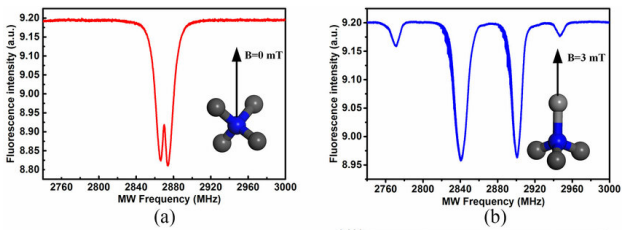

Figure 11. ODMR fluorescence spectra showing the single resonance dip at 2.87 GHz at zero field (left) and the Zeeman-split double dip under an applied magnetic field (right). (Ma et al., 2019)

While a single NV center can precisely measure the field strength via Equation 6, it is highly directional; the $\cos(\theta)$ term means it only detects the parallel field projection. Because of the diamond crystal's tetrahedral bonding, NV centers naturally align along four possible crystallographic directions: [111], [1$\bar{1}\bar{1}$], [$\bar{1}$1$\bar{1}$], and [$\bar{1}\bar{1}$1], as illustrated in Fig. 12.

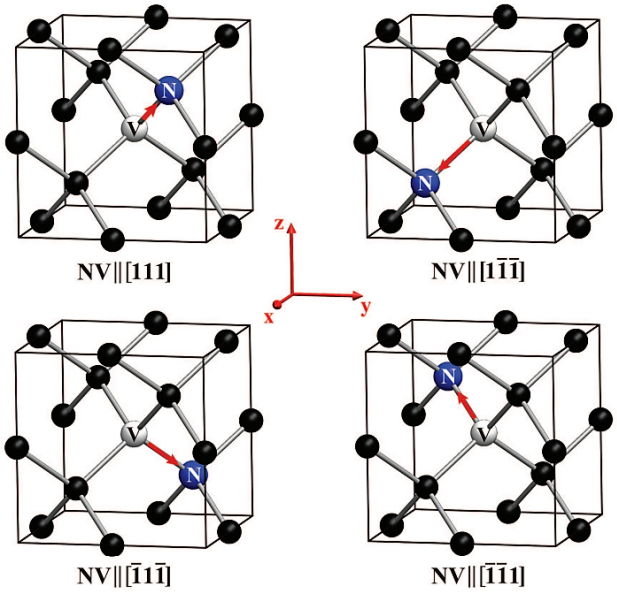

Figure 12. The four possible crystallographic orientations of the NV center axis in the diamond lattice, aligned along the ⟨111⟩ family of directions.

To measure the full 3D direction of a magnetic field, engineers utilize an ensemble of NV centers, a bulk volume of diamond containing millions of defects distributed across all four orientations. An external magnetic field intercepts each of these four axes at a different angle, so each orientation group experiences a different parallel field projection, leading to four unique degrees of Zeeman splitting.

When the fluorescence of the entire ensemble is collected, the ODMR spectrum reveals eight distinct dips, four pairs of peaks, each corresponding to one of the NV axes (NV1, NV2, NV3, and NV4). By measuring the relative peak separations of these four pairs, both the absolute magnitude and the exact 3D directional vector of the magnetic field can be fully reconstructed, as shown in Fig. 13.

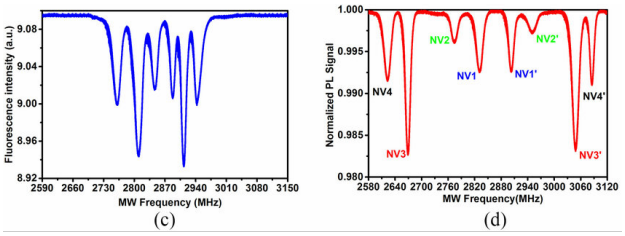

Figure 13. Ensemble ODMR spectrum showing eight distinct resonance dips corresponding to the four NV orientations (NV1–NV4). (Ma et al., 2019)

4. FABRICATION

4.1. Diamond Growth

To harness NV centers for precision quantum applications, the host diamond matrix must be engineered with extreme purity. Historically, synthetic diamonds have been produced using High-Pressure High-Temperature (HPHT) methods, which mimic the extreme thermodynamic conditions of the Earth's mantle. While HPHT is highly effective for creating industrial abrasives, it incorporates metallic flux inclusions and uncontrollable clusters of nitrogen, which severely degrade electron spin coherence. Consequently, quantum-grade diamond is almost exclusively synthesized using Microwave Plasma Chemical Vapor Deposition (MPCVD), a process that builds the crystal lattice atom by atom from a highly purified gas phase.

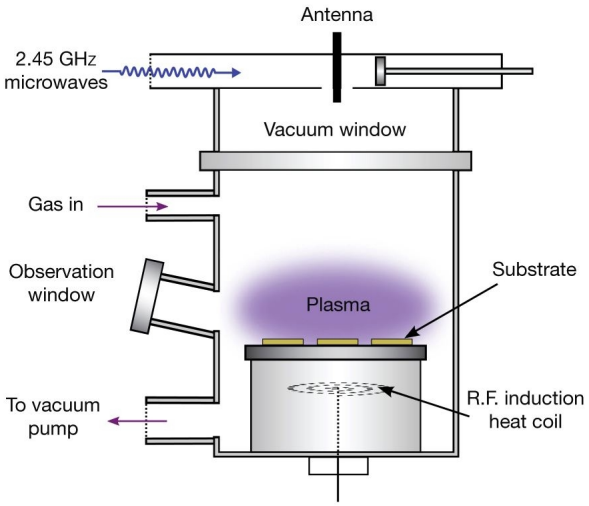

Figure 14. Interior view of an MPCVD chamber during diamond growth, showing the microwave-ignited hydrogen–methane plasma above the diamond substrate.

Inside the MPCVD vacuum chamber, high-power microwaves ignite a precursor mixture of hydrogen (H_2) and a small fraction of methane (CH_4) into a plasma. The intense energy cracks these molecules into highly reactive radicals. The atomic hydrogen radicals play a crucial dual role: they stabilize the surface by terminating dangling bonds and selectively etch away any weakly bonded sp^2 graphitic carbon, ensuring only the rigid sp^3 diamond lattice survives.

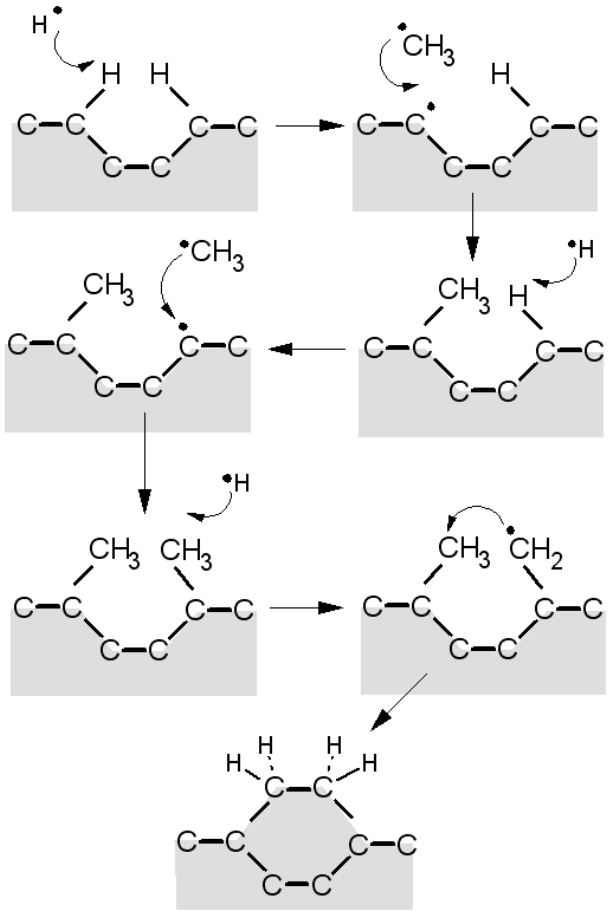

Figure 15. Schematic of the epitaxial diamond growth cycle at the substrate surface, illustrating hydrogen abstraction, radical addition, and selective sp^2 etching.

Epitaxial growth occurs through a continuous chemical cycle at the substrate surface. Atomic hydrogen from the plasma strips a terminating hydrogen atom from the diamond, leaving a highly reactive open site. A cracked methane radical (such as CH_3) immediately bonds to this site, sequentially building the lattice layer by layer. Because this atom-by-atom assembly must be meticulously controlled to ensure extreme quantum purity, the typical growth rate is relatively slow, generally ranging from 1 to 10 μm per hour. During this process, trace amounts of nitrogen gas (N_2) can be precisely bled into the chamber for "in-situ" doping. This natively incorporates single substitutional nitrogen atoms into the expanding matrix, perfectly setting the stage for targeted NV center creation in the next processing steps.

4.2. Defect Creation and Activation

After the MPCVD growth phase, the diamond lattice may contain nitrogen, but it lacks the critical missing component: the vacancies. In quantum manufacturing, this defect activation is typically achieved through one of two primary methods: electron irradiation or nitrogen ion implantation.

4.2.1. *Electron Irradiation*

For diamonds doped with nitrogen "in-situ" during growth, vacancies are created via high-energy electron irradiation. These light, energetic electrons knock carbon atoms out of their lattice sites, penetrating deeply and uniformly into the bulk diamond with minimal collateral damage.

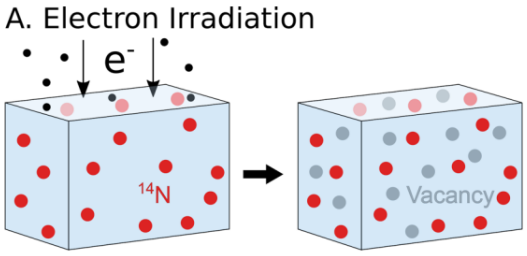

Figure 16. Diamond lattice before and after electron irradiation. (Ruf et al., 2019)

While excellent for creating pristine bulk sensors, this method lacks spatial control. Vacancies are generated randomly throughout the crystal, meaning this approach cannot be used to place NV centers in targeted nanoscale arrays.

4.2.2. *Nitrogen Ion Implantation*

Alternatively, for diamond grown without nitrogen dopants, engineers use nitrogen ion implantation. A particle accelerator shoots heavy nitrogen ions into the diamond, simultaneously delivering the nitrogen impurity and creating vacancies upon impact. While this method offers spatial precision, allowing engineers to "write" NV centers into exact geometric arrays using masks, the heavy ions can shatter the local lattice, creating unwanted defect clusters, and their penetration depth is highly constrained, as shown in Fig. 17.

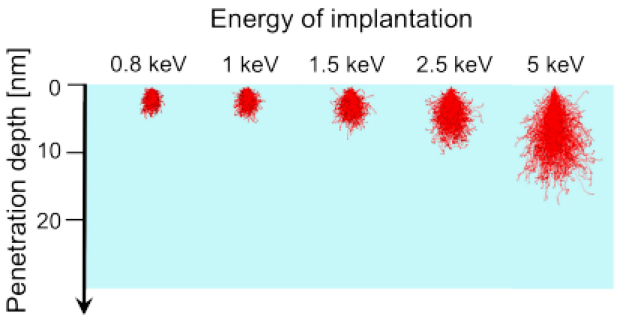

Figure 17. Implantation depth profiles of nitrogen ions in diamond as a function of accelerating energy. (Haque & Sumaiya, 2017)

4.3. Post-Processing and Charge Stabilization

Regardless of the activation method employed, both techniques require a subsequent thermal annealing step, typically performed at 800–1000°C in an inert atmosphere. This provides the vacancies with sufficient thermal energy to diffuse through the lattice and pair with a substitutional nitrogen atom, completing the formation of the NV center.

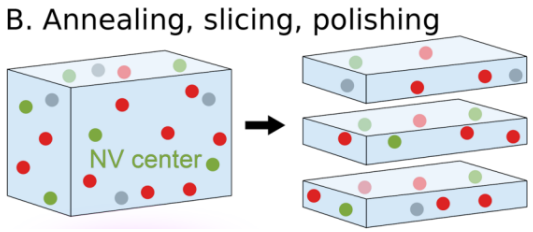

Figure 18. Post processing steps for NV center diamonds. (Ruf et al., 2019)

To function as a sensor, the newly formed defect must be locked into its magnetically sensitive negative charge state (NV^-). The diamond undergoes oxygen surface termination, typically via oxygen plasma or acid wash, capping the surface carbon bonds with highly electronegative oxygen atoms. This bends the local energy bands, repelling electrons inward to stably trap the extra electron at the NV site.

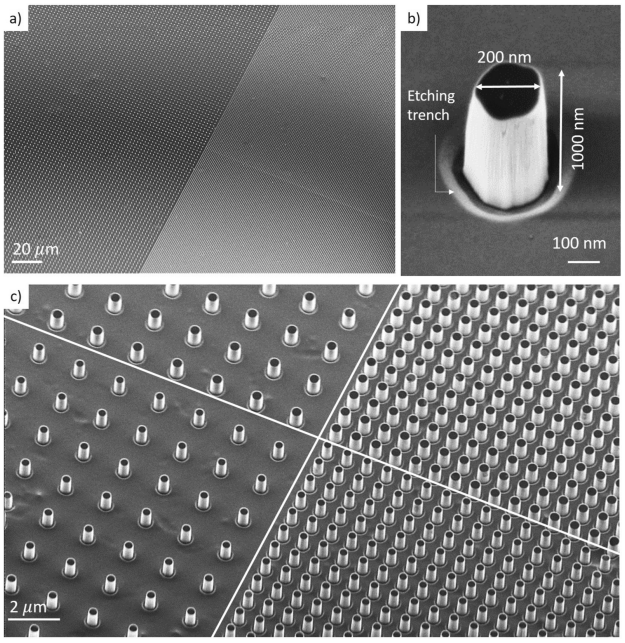

Figure 19. Scanning electron microscope (SEM) image of diamond nanopillars. (Losero et al., 2023)

Finally, because diamond's high refractive index traps much of the emitted fluorescence via total internal reflection, the crystal surface must be physically sculpted. Engineers etch specialized optical structures, such as solid-state nanopillars or photonic cavities, directly into the diamond. These nanoscale waveguides efficiently channel the light outward, enhancing both the optical collection efficiency and the spatial resolution of the sensor.

5. TECHNOLOGY LANDSCAPE AND FUTURE OUTLOOK

5.1. Applications

Because NV centers combine atomic-scale spatial resolution with extraordinary magnetic sensitivity at room temperature, they unlock applications that are fundamentally impossible for traditional sensors. In the realm of biophysics, NV centers enable completely non-destructive nanoscale biosensing. Because the diamond lattice is biologically inert and non-toxic, living cells can be cultured directly on the sensor's surface.

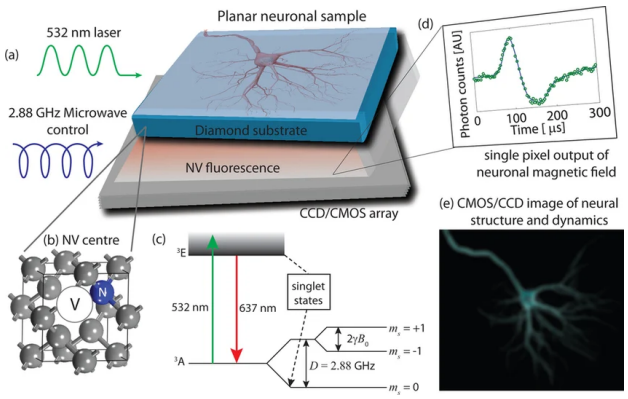

Figure 20. Schematic of an NV center-based neural imaging system, showing a diamond substrate doped with NV centers beneath a neural network component, with 532 nm excitation and widefield fluorescence readout via a CMOS camera. (Le Sage et al., 2012)

As shown in Fig. 20, a neural network component such as an axon can be placed directly on a diamond substrate doped with NV centers. By applying a 2.88 GHz microwave field and 532 nm optical excitation, the NV spin state becomes directly dependent on the highly localized magnetic field produced by the axon. The red fluorescence is then continuously monitored using a CMOS or CCD camera. By tracking the intensity across many pixels, engineers can generate a dynamic, widefield image of neural dynamics, theoretically capable of detecting the incredibly faint ~0.2 nT magnetic signature of a single firing mammalian action potential.

Beyond the nanoscale, bulk ensembles of NV centers are being actively developed for macro-scale navigation. Because they operate entirely solid-state and require no external calibration signals, NV magnetometers are prime candidates for Magnetic Navigation (MAGNAV).

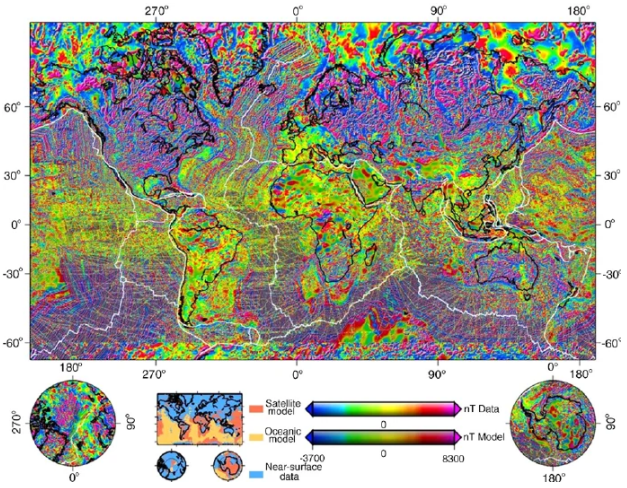

Figure 21. World Magnetic Anomaly Map showing localized crustal magnetic field variations that can serve as a natural navigation reference for GPS-denied environments. (Khorhonen et al. 2007)

By mapping the Earth's localized crustal magnetic anomalies, as shown in Fig. 21, these sensors can provide highly accurate GPS-denied navigation. This offers a robust, unjammable alternative to vulnerable satellite systems, useful for deep-sea exploration where GPS signals cannot penetrate.

While the fundamental physics of these applications is proven, a significant engineering challenge remains in transitioning these systems from optics-heavy lab benches to field-deployable devices. A major frontier in this effort is the heterogeneous integration of quantum diamond with mature photonic and electronic platforms, such as CMOS circuits and integrated waveguides, to drastically shrink the footprint of the optical readout and microwave delivery systems.

5.2. Benchmarking Against Existing Technologies

NV magnetometers bridge a critical gap in magnetic sensing, offering a unique balance of sensitivity, operating conditions, and spatial resolution compared to current gold standards.

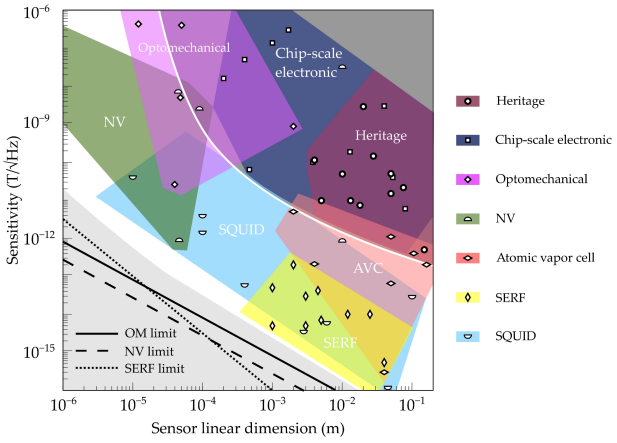

Figure 22. Benchmarking plot of magnetic field sensitivity versus sensor size for various magnetometer technologies, as well as their theoretical limit. (Bennett et al., 2021)

As shown in Fig. 22, Superconducting Quantum Interference Devices (SQUIDs) and Spin-Exchange Relaxation-Free (SERF) vapor cells offer extreme sensitivity down to the femtotesla level. However, they require significant logistical support, bulky cryogenic cooling for SQUIDs, or strict heating and magnetic shielding for SERF cells. Furthermore, their macroscopic nature limits their spatial resolution to measuring bulk average fields. On the other end of the spectrum,

Table 2. Technical Comparison of Magnetometer Technologies

	NV Center	SQUID	Vapor Cell	Hall Sensor
Mechanism	ODMR spin readout	Flux quantization	Larmor precession (OPM)	Lorentz force
Sensitivity	~1–100 pT/$\sqrt{\text{Hz}}$	~0.001–0.01 pT/$\sqrt{\text{Hz}}$	~0.01–0.1 pT/$\sqrt{\text{Hz}}$	~1 μT/$\sqrt{\text{Hz}}$
Spatial Res.	1–100 nm	10 μm–1 mm	1 mm–1 cm	10–100 μm

Table 3. Practical Comparison of Magnetometer Technologies

	NV Center	SQUID	Vapor Cell	Hall Sensor
Operating Temp.	Room temp.	Cryogenic (~4 K)	Heated (300–450 K)	Room temp.
Cost	Moderate–High	Very High	Moderate	Very Low
Scalability	High	Low	Moderate	Very High
Deployment	Solid-state, compact	Bulky, cryostat required	Shielding required	Fully integrated

Sensitivity values quoted for single-pixel or single-sensor operation under standard conditions.

traditional solid-state Hall effect sensors are cheap and operate at room temperature, but completely lack the sensitivity required for quantum or biological measurements.

The NV center uniquely resolves these trade-offs. It delivers extraordinary magnetic sensitivity and nanoscale spatial resolution while remaining entirely solid-state and operating at ambient room temperature. By eliminating the need for cryogenics, heating elements, or vacuum enclosures, NV centers provide a robust, highly precise platform for real-world deployable sensors.

5.3. Current Engineering Bottlenecks and Challenges

While the fundamental physics of the NV center are well-established, transitioning the technology from laboratory optical benches to ubiquitous, commercially viable sensors requires overcoming several severe engineering bottlenecks.

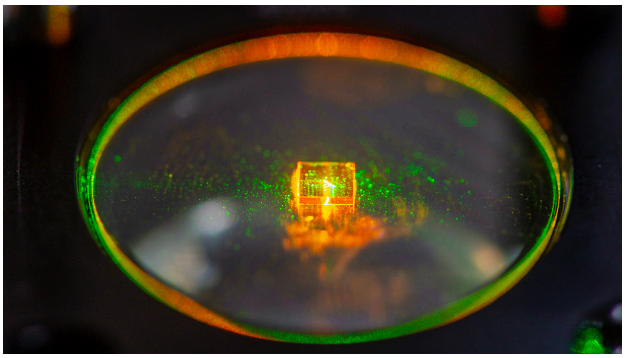

Figure 23. A commercially available quantum-grade diamond with implanted NV^- centers, illustrating the early-stage commercialization of NV-based sensing platforms.

5.3.1. Diamond Growth and Fabrication Limits

The most fundamental barrier to commercial scaling is the host material itself. As discussed previously, quantum-grade diamond requires extreme isotopic purity, meaning growth via MPCVD is exceptionally slow, often yielding only micrometers per hour, and prohibitively expensive. Furthermore, diamond's legendary hardness and chemical inertness make it notoriously difficult to process. Etching precise nanostructures, such as the pillars and waveguides needed for efficient light extraction, requires highly specialized, aggressive plasma chemistries that do not easily integrate with standard semiconductor nanofabrication workflows.

5.3.2. Surface Decoherence

For applications requiring maximum spatial resolution, such as nanoscale biosensing, NV centers must be implanted within just a few nanometers of the diamond surface. However, this proximity exposes the sensitive electron spins to a chaotic environment of dangling carbon bonds, surface oxides, and fluctuating charge traps. This magnetic surface noise rapidly scrambles the electron spin state, causing severe decoherence and drastically reducing the sensor's sensitivity. Promising mitigation strategies include surface termination engineering and atomic layer deposition of protective oxide coatings to passivate these noise sources.

5.3.3. Charge State Instability

Even if perfectly fabricated, the NV center suffers from dynamic instability during operation. The sensor relies exclusively on the negatively charged NV^- state to provide the $S = 1$ spin triplet necessary for ODMR. However, under the continuous 532 nm optical illumination required to read the sensor, the defect can photo-ionize, spontaneously losing its extra electron and converting into the neutral NV^0 state. Because NV^0 has a different spin structure ($S = 1/2$) and lacks the crucial zero-field splitting, it is effectively "magnetically blind," heavily degrading the overall optical contrast. Active research into engineered Fermi level pinning and band-structure engineering via controlled surface termination aims to stabilize the NV^- charge state under continuous illumination.

6. CONCLUSION

The nitrogen-vacancy (NV) center in diamond represents a highly versatile platform for next-generation quantum sensing. By leveraging the Zeeman effect and Optically Detected Magnetic Resonance (ODMR), NV centers provide exceptional magnetic sensitivity and atomic-scale spatial resolution while operating entirely at room temperature in a solid-state environment. While significant manufacturing bottlenecks remain regarding pure diamond synthesis, surface decoherence, and charge state instability, the push toward heterogeneous integration offers a practical pathway to mitigate these challenges. Ultimately, the successful transition of NV technology from laboratory optical setups to scalable, chip-integrated architectures may enable broader deployment in fields ranging from nanoscale biological imaging to GPS-denied magnetic navigation.

REFERENCES

[1] D. Le Sage et al., "High spatial and temporal resolution wide-field imaging of neuron activity using quantum NV-diamond", *Scientific Reports*, vol. 2, p. 401, 2012. DOI: 10.1038/srep00401

[2] A. Faraon, C. Santori, Z. Huang, V. M. Acosta, R. G. Beausoleil, and P. E. Barclay, "Lifetime reduction and enhanced emission of single photon color centers in nanodiamond via surrounding refractive index modification", *Scientific Reports*, vol. 5, no. 1, p. 11 179, 2015. DOI: 10.1038/srep11179

[3] S. Sharma, C. Hovde, D. H. Beck, and F. Alghannam, "Imaging strain and electric fields in NV ensembles using Stark shift measurements", University of Illinois / Southwest Sciences / Texas A&M University, Tech. Rep., Dec. 2017.

[4] W. Ma et al., "High-sensitivity three-axis vector magnetometry using the electron spin ensembles in single diamond", *IEEE Magnetics Letters*, 2019. DOI: 10.1109/LMAG.2019.2891616

[5] M. Ruf et al., "Optically coherent nitrogen-vacancy centers in micrometer-thin etched diamond membranes", *Nano Letters*, vol. 19, pp. 3987–3992, 2019. DOI: 10.1021/acs.nanolett.9b01298

[6] G. Thiering and A. Gali, "Color centers in diamond for quantum applications", in *Semiconductors and Semimetals*, vol. 103, Elsevier, 2020, pp. 1–36. DOI: 10.1016/bs.semsem.2020.03.001

[7] J. S. Bennett et al., "Precision magnetometers for aerospace applications: A review", *Sensors*, vol. 21, no. 16, p. 5568, 2021. DOI: 10.3390/s21165568

[8] T. F. Segawa and R. Igarashi, "Nanoscale quantum sensing with nitrogen-vacancy centers in nanodiamonds – A magnetic resonance perspective", *Journal of Magnetic Resonance*, vol. 345, p. 107 315, 2022. DOI: 10.1016/j.jmr.2022.107315

[9] E. Losero et al., "Neuronal growth on high-aspect-ratio diamond nanopillar arrays for biosensing applications", *Scientific Reports*, vol. 13, p. 5909, 2023. DOI: 10.1038/s41598-023-32941-3

[10] Z. Fan, L. Xing, F. Wu, X. Feng, and J. Zhang, "The optimization of microwave field characteristics for ODMR measurement of nitrogen-vacancy centers in diamond", *Photonics*, vol. 11, no. 5, p. 436, 2024. DOI: 10.3390/photonics11050436

[11] C. M. Knaut et al., "Entanglement of nanophotonic quantum memory nodes in a telecom network", *Nature*, vol. 629, pp. 573–578, 2024. DOI: 10.1038/s41586-024-07252-z

[12] R. A. Parker et al., "A diamond nanophotonic interface with an optically accessible deterministic electronuclear spin register", *Nature Photonics*, vol. 18, pp. 156–161, 2024. DOI: 10.1038/s41566-023-01384-1

[13] Y. Li, H. Li, T. Yi, C. Li, and J. Wei, "A review of the study of diamond NV color centers: Fabrication, application and challenge", *Functional Diamond*, vol. 5, no. 1, p. 2 567 286, 2025. DOI: 10.1002/fd.2567286